Sumerianz Journal of Scientific Research, 2023, Vol. 6, No. 1, pp. 14-26
ISSN(e): 2617-6955, ISSN(p): 2617-765X
Website: https://www.sumerianz.com
DOI: https://doi.org/10.47752/sjsr.61.14.26

Original Article Open Access

Monte-Carlo Calculations (GEANT4) of Ions Resulting of the Irradiation and Interaction of a Static Electric Field and Some Experimental Tests – an Attractive Way to Improve the Enhancement of the Yield of Hydrogen

W. Ulmer*
Gesellschaft für Qualitätssicherung in der Medizin, Deizisau, MPI of Physics, Göttingen, Germany
The process of patent registration at European Patent Office (EPO 20 154 617.3) has successfully been finished and already made public by the office
Email: waldemar.ulmer@gmx.net

U. Ulmer
Technische Hochschule Nürnberg, Germany
The process of patent registration at European Patent Office (EPO 20 154 617.3) has successfully been finished and already made public by the office

Article History
Received: 10 December 2022
Revised: 21 February 2023
Accepted: 25 February 2023
Published: 28 February 2023

How to Cite
Ulmer, W. and Ulmer, U., 2023. "Monte-Carlo Calculations (GEANT4) of Ions Resulting of the Irradiation and Interaction of a Static Electric Field and Some Experimental Tests – an Attractive Way to Improve the Enhancement of the Yield of Hydrogen." *Sumerianz Journal of Scientific Research*, vol. 6, pp. 14-26.

Abstract
The past decade has emerged a growing interest in the electrolysis and Hydrogen technology as a surrogate of the conventional energy sources. Many novel materials have been tested to improve the Hydrogen yield and to reach a breakthrough with them. In the present analysis the electrolysis with additional 6 MV ionizing radiation produced by a linear accelerator has been tested in order to suggest γ-radiation of radioactive waste of nuclear reactors and other sources, which is the goal of this study. For this purpose, a box consisting of laboratory glass filled with water and capacitors as electrodes has been used for the performance of the tests. The experimental tests have provided significant differences of the Hydrogen release, if the test phantom has been subjected to radiation and the comparison without it. A theoretical insight obtained by the consideration an extension of the diffusion equation by a static electric field in order to describe the transport of ions. Quantitative examinations have been made possible by Monte Carlo calculations with GEANT4, which provided good agreement with experimental data, since this code is also applicable by inclusion of external electric and magnetic fields.
Keywords: Electrolysis; Enhancement hydrogen production via ionization radiation; Use of radioactive waste; Monte carlo calculations with GEANT4.

1. Introduction
Since the supply with sufficient energy incorporates a world-wide task, the emphasis of the Hydrogen production has become increasing importance. A well-known physicochemical process, namely the Hydrogen electrolysis, has reached the focus interest in various studies. The goal of this analysis is the application of the radioactive waste as an alternative way to provide the energy for water hydrolysis in order to enhance the yield of Oxygen. The most important isotope in radioactive waste is Cs^{137} with a half-time of 30 years, but due to the extreme activity various half-times are required until the intensity of the radiation emitted by this isotope is decreased enough so that it can be handled by usual technical methods. In order to avoid this long-time and unpredictable storage of Cs^{137} , there have been elaborated some concepts, which will be mentioned in the final section. At this place, we should like to note, that the keywords '***Radioactive waste – new exploitation technologies'*** provide various references in the internet. Therefore, a listing of them seems not to be necessary. In order to test the proposal by

suitable measurements, the bremsstrahlung of 6 MV of a linear accelerator has been used with regard to a suitable phantom. In addition, Monte-Carlo calculations with the code GEANT4 have been carried out and confirmed the measurement results. These calculations offer further options to alter and optimize the phantom geometry in order to optimize the hydrolysis process and yield of H_2, which will be discussed in section 5.

2. Methods

2.1. Experimental Configuration

The experimental tests have been carried out with a phantom (aquarium) consisting of laboratory glass delivered by Mollenkopf GmbH, Stuttgart. The phantom length and height amounted to 18 cm and the breadth to 13 cm filled with two-fold distilled water and 50 g/2.5 L NaOH. The walls along the radiation propagation have been equipped with noble steel (capacitors), thickness 1 mm connected with a power supply for the cathode and anode. In the middle part of the phantom a diaphragm has been allocated to reach a better separation of the Hydrogen and Oxygen production. The tests have been performed at a linear accelerator (usual abbreviation: Linac) of the company Elekta, Great Britain, in the center of Radio-Oncology in Munich, Maximilian Platz 2.

Figures 1, 2 present the measurement configuration, and Figure 3 shows the dose distribution, correlated to the corresponding ion concentration produced by 6 MV bremsstrahlung. The experimental tests have been carried out with 10 x 10 cm^2 field size at the isocenter. Opposing radiation is, however, not possible by this condition.

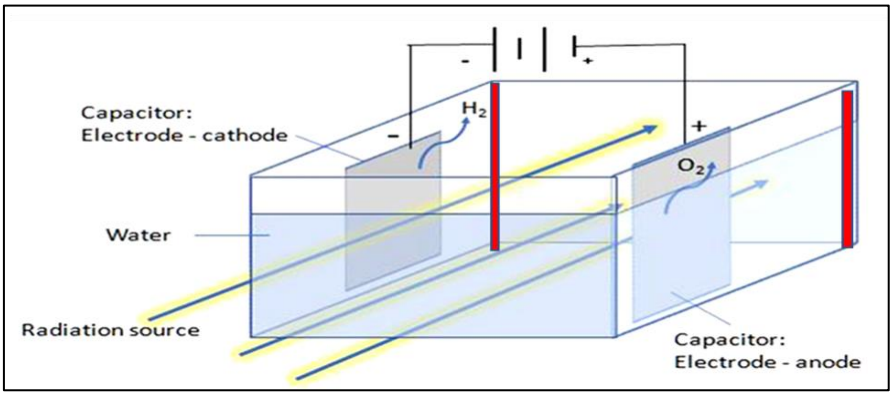

Figure-1. Basic configuration of an electrolyzer using external γ-rays or bremsstrahlung and two capacitors for cathode and anode at the walls of the phantom. The two conventional electrodes (represented **by red color**) concepted as solenoids of noble steel (diameter: 0.7 cm) have been placed by sufficient distances from the capacitors. In this way, the mutual influence could be prevented

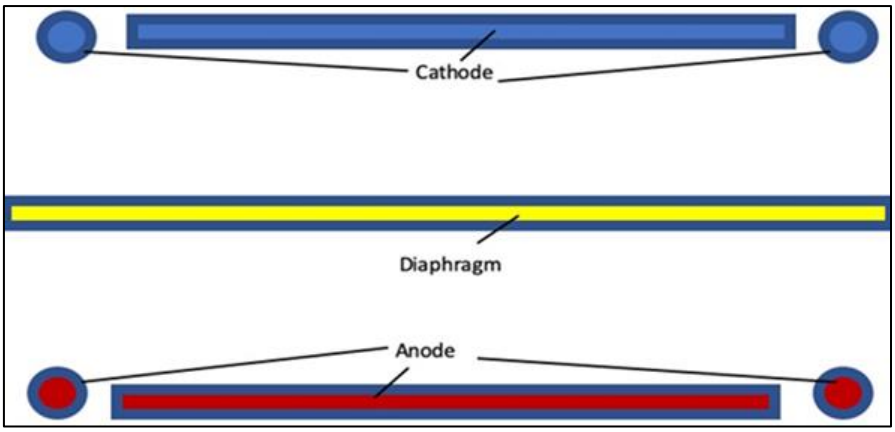

Figure-2. Top view on an electrolyzer with the capacitor plates and additional electrodes. The use of a diaphragm is optional and serves for separation of H_2 and O_2 gases to avoid the formation of explosive gas mixtures. This configuration was used during all measurement series

As already mentioned, opposite irradiation is impossible by a Linac, the depth dose curves for 6 MV bremsstrahlung only can show the characteristic behavior as given in Figure 3. In section 5 the configuration of a corresponding apparatus suitable for the application of radioactive sources (e. g. waste of nuclear reactors) will be analyzed, and the irradiation occurs by two opposite sources. By that, the distributions of dose and ions can better approximately assume homogenous properties.

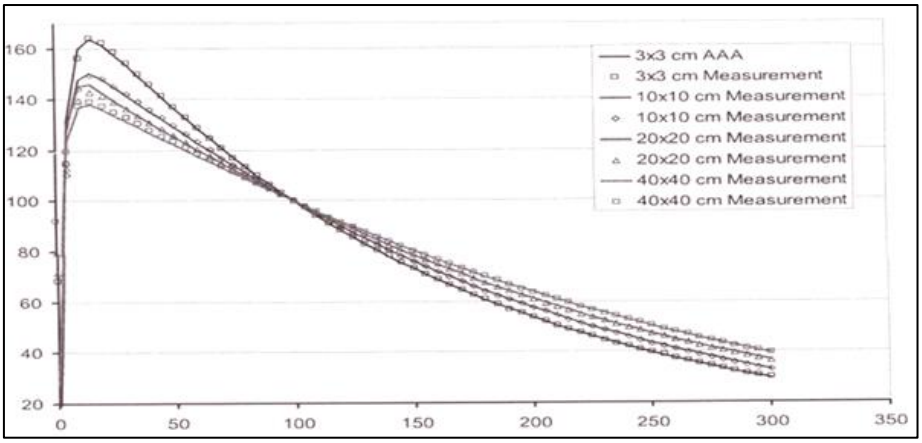

Figure-3. Depth dose curves of 6 MV 'bremsstrahlung' of a Linac [1] depending on field size

2.2. Properties of Electrolizers and Ionizing Radiation

Since Hydrogen (H_2) based on electrolyzers (usual technical terminus) is becoming of growing importance for two closely related, well-known reasons, namely the reserves of fossil fuel are continuously decreasing, and the combustion of these fossil fuels has evoked severe environmental problems through the release of carbon dioxide (CO_2) and other harmful gases. The principle of electrolytic water decomposition to gain H_2 and Oxygen (O_2) using electric energy is an old procedure in electrochemistry. The principle of the well-known electrolytic water splitting is presented schematically in Figure 4. Therefore, the discussion of details is superfluous, and we restrict us to the final reaction in eq. (1):

$$\mathbf{2 \cdot H_2O + Energy\vec{}_{(catalyst)} 2 \cdot H_2 + O_2.} \qquad \mathbf{(1)}$$

The source of energy is usually provided by an electric power supply to drive the water splitting reaction. Theoretically, the minimum voltage for water splitting amounts to 1.23 V, but, in practice, higher voltages are required to overcome kinetic and other limitations, e., g. the electric field strength between the poles decreases with their increasing distance.

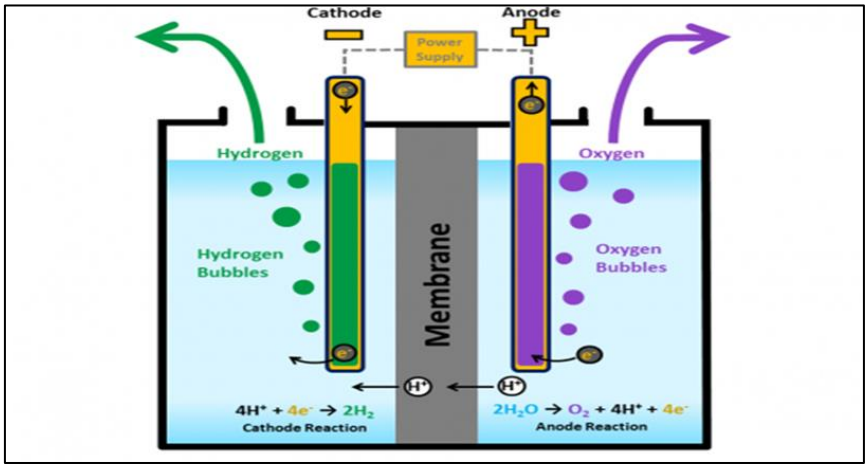

Figure-4. Schematic representation of the water electrolysis – the complete apparatus is referred to as electrolyzer [2-4]

The electric energy required to drive the water splitting reaction incorporates a major limitation of the production of H_2 by electrolysis. This limitation results from the significant cost for electricity, and impeding their economic operation. In this invention, we present an apparatus that is capable to *utilize ionizing radiation to reduce the amount of electric energy necessary to initiate the water splitting reaction*. Hereby, ionizing radiation is introduced into a modified electrolyzer apparatus to decompose water (Figure 4). The radiation can also originate from the decay reactions of radioactive substances (e. g. nuclear waste of nuclear reactors) or naturally occurring radiation can be taken into account. By that, effectively excites water molecules into excited and ionized states, which facilitates their decomposition into H_2 and O_2 gases at electrode surfaces. *Aten-fold increase of H_2 production yield has been detected in the presence of ionizing radiation*, relative to the same experimental conditions by the absence of ionizing radiation.

2.3. Monte-Carlo Calculations with GEANT4

The Monte Carlo code GEANT4-Documents [5] is a wide-spread and accurate tool with respect to all radiation applications, including nuclear and high energy physics, since it permits the additional features like electric and magnetic fields in order to manipulate the behavior of charged particles and neutrons. In this study, we preferably think of electric fields produced by the capacitor and further electrodes. The additional use of magnetic fields will be considered in the final section. These fields are necessary for the separation of ions. In the outlook regarding more

sophisticated realizations of the technical equipment the additional inclusion of inhomogeneous magnetic fields will be taken into consideration.

In this communication, we have applied this code with regard to the configuration in Figures 1, 2, 3, i.e., the ionization produced by 6 MV in an aquarium and an additional electric based on Figure 4 and realized by capacitors at the phantom walls. The advantage of MC calculations is given by readily modified geometrical alterations, which would require to completely new apparatus constructions. A further advantage of GEANT4 is, that the code permits the inclusion of radioactive substrates as waste of nuclear reactors, which represent the goal of this study.

2.4. Theoretical Principles: Some Thermodynamical Aspects and the Role of Ionizing Radiation Interacting with a Static Electric Field Described by a Generalized Diffusion Equation

Thermodynamically, the water splitting reaction is an uphill reaction. A minimum amount of 571.8 kJ mol^{-1} must be supplied to drive this reaction according to eq. (2).

$$\left.\begin{array}{l} \mathbf{2 \cdot H_2O + \Delta H^0 \rightarrow 2 \cdot H_2 + O_2} \\ \mathbf{\Delta H^0 = 571.8 kJ/mol} \\ \mathbf{\tau = 15^0 C; P(pressure) = 1013 Pa} \end{array}\right\}. \quad (2)$$

This energy can be supplied in the form of electricity, light, e., g., radiation, or heat. When photons of sufficient energy level (h•ν) interact with water molecules, this can result in the formation of excited states, according to eq. (3):

$$\mathbf{H_2O + h \cdot \nu \rightarrow H_2O_{excited\ state.}} \qquad (3)$$

The nature of the excited state of the water molecule depends on the energy level of the incident photon (E_{photon}). The ionization energy of H_2O amounts to 12 eV in the gaseous state, whereas in fluid form it mainly depends on the temperature and eventually on a further solvent, in general about 9 eV. If E_{photon} exceeds the energy required to ionize the water molecule (E_{ion}), i.,e. E_{photon} > (or >>) E_{ion}, then an electron can be ejected from the water molecule. A water cation and a free electron are released according to eq. (4).

$$\mathbf{H_2O + h \cdot \nu (E_{photon} > E_{ion}) \rightarrow H_2O^+ + e^- + E_{kin}}. \quad (4)$$

This effect is referred to as the Einstein photo effect. If such a situation occurs, the collision of the released electron with H_2O-molecules in its environment can lead to the ionization of additional water molecules according to eq. (5):

$$\mathbf{H_2O + e^- \rightarrow H_2O^+ + 2 \cdot \tilde{e}^-} \quad . \qquad (5)$$

The notation $\tilde{e}^-$ in eq. (5) indicates that the kinetic energy of the two released electrons is lower than that of the impinging electron $\mathbf{e^-}$. If the photon energy E_{photon} > 15 keV or >> 15 keV a similar physical process occurs, known as Compton effect. Here, the energy level of the incident photon γ is so high that its collision with a water molecule causes the ejection of an electron e^- and the additional ejection of a 'recoil' photon, γ', as shown in eq. (6).

$$\mathbf{h\nu_\gamma + H_2O \rightarrow h\nu_{\gamma'} + e^- + H_2O^+}. \quad (6)$$

If the energy level of the recoil photon is sufficient, then this photon can excite an additional water molecule. The whole procedure can be repeated numerous times until the energy level of the recoil photon is sufficiently low, which means that the Einstein photo-effect still occurs.

Usual Roentgen rays with energy E_{photon}> 15 keV or >> 15 keV and γ-quanta with photon energies E_{photon} in the MeV domain can only lose their energy by Compton interaction. The energy balance of one collision interaction is given by:

$$\mathbf{E_\gamma = E_{\gamma'} + E_{electron}} \quad . \qquad (7)$$

In addition to the recoil photons, the released electrons due to each Compton process is itself capable to ionize various H_2O-molecules by the electron scatter.

With regard to the Compton process, we should like to list some further important reactions with photons and released electrons according to eq. (8):

$$\left.\begin{array}{l} \mathbf{\gamma + H_2O \rightarrow OH \bullet + H \bullet + \gamma'} \\ \mathbf{\gamma + H_2O + e^- \rightarrow OH \bullet + H \bullet + \gamma' + e^-} \\ \mathbf{H_2O + e^- \rightarrow OH \bullet + H \bullet + e'^-} \end{array}\right\}. \quad (8)$$

The of **H·** and **OH·** represent radical states, and **e'⁻** refers to a recoil electron with lower energy compared to the preceding electron e^- before scatter. A variety of possible reactions and interactions can occur during the collision of photons with water moleules, all of which lead to the formation of excited states. These excited states are important intermediates of the overall water splitting reaction (see e. g,, eq. 8). Ionizing radiation effectively increases the density of excited states as compared to the absence of ionizing radiation.

2.4.1. Generalized diffusion Equation by Inclusion of an Electric Field

The physical process can qualitatively be described by diffusion of the scattered electrons with the help of the following diffusion equation subjected to an electric field produced by a cathode and anode used by plates (capacitor) at the wall of the aquarium:

$$\mathbf{- \partial C/\partial t + D \cdot \Delta C + \alpha \cdot y \cdot C = 0} \quad . \qquad (9)$$

Eq. (9) represents the well-known diffusion equation in 3 dimensions extended by an electric field [6].

The factor α is given by either $F \cdot e_0 \cdot (U/d)/\hbar$ with F: Faraday constant and e_0 elementary charge or by $Q \cdot (U/d)/\hbar$ with Q as the total charge of the medium produced by radiation. Further abbreviations are D: diffusion constant; U: voltage; d: distance between the plates of the capacitor and $\hbar$: Planck's constant divided by 2π. The electric field strength results from U/d = |**E**|.

The above stated parameters result from the transition of an electric field with ionization densities in the electric field with the Schrödinger equation, if the time-derivative is imaginary, and the substitution $t \rightarrow i \cdot t$ is performed.

The diffusion constant D has to satisfy the Einstein-Smoluchowski relation:

$$D = k_B \cdot T/(6\pi \cdot \eta \cdot r). \quad (10)$$

The parameters of eq. (10) are given by T: absolute temperature, k_B: Boltzmann constant, η: viscosity of the medium and r: ion radius. The following numerical values can be assumed: The viscosity η of H_2O is η = 1 at 20° C and η = 0.891 at 25° C. The ion radius r of H (proton) is $r = 0.85 \cdot 10^{-13}$ cm and of Oxygen it amounts to about $r \approx 6 \cdot 10^{-13}$ cm. The proportionality between diffusion constant D and temperature T is an essential feature in the present analysis, as it could be exploited to improve the yield of Hydrogen.

The above equation is solved by '**ansatz**' according to eq. (11):

$$C = A \cdot \exp[(i \cdot (k_1 x + k_2 y + k_3 z)] \exp(\gamma \cdot t \cdot y) \exp[(-(\tau_1 t + \tau_2 t^2 + \tau_3 t^3)] \ . \ (11)$$

The parameters of this equation have to satisfy the following conditions:

$$\alpha = \gamma; \quad (12a)$$

$$\tau_1 = D \cdot (k_1^2 + k_2^2 + k_3^2); \quad (12b)$$

$$\tau_2 = i \cdot D \cdot k_1 \cdot \gamma; \ \tau_3 = D \cdot \gamma^2. \quad (12c)$$

Due to the linearity of the above equation, the integration over the vector **k** leads to the integral (13):

$$C = \iiint A \cdot \exp[(i \cdot (k_1 x + k_2 y + k_3 z)] \exp(\alpha \cdot t \cdot y) \cdot \exp[(-(\tau_1 t + \tau_2 t^2 + \tau_3 t^3)] dk_1 dk_2 dk_3. \quad (13)$$

The solution of this integral is given by:

$$C = N \cdot \exp[-((y - D \cdot \alpha \cdot t^2)^2 + x^2 + z^2)/(4 \cdot D \cdot t)] \cdot \exp(\alpha \cdot y \cdot t) \cdot \exp(-D \cdot \alpha^2 \cdot t^3/3). \quad (14)$$

$$\text{The normalization constant N is given by: } 1/(4 \cdot \pi \cdot D \cdot t)^{3/2}. \quad (15)$$

For the reason of symmetry of the capacitor a further solution exists, namely by replacing x by **y' = d-y**:

$$C = N \cdot \exp[-((y' - D \cdot \alpha \cdot t^2)^2 + x^2 + z^2)/(4 \cdot D \cdot t)] \cdot \exp(\alpha \cdot y' \cdot t) \cdot \exp(-D \cdot \alpha^2 \cdot t^3/3). \quad (16)$$

The normalization factor N according to eq. (15) remains unchanged.

Eq. (11) can be solved exactly, but by taking account of some wall restriction given by the electric field produced in the capacitor, the solution (16) represents a rather satisfactory solution property.

The resulting ion concentration profiles are plotted in Figures 5 and 6. Figures 5 shows the distribution at the beginning of the experiment, immediately after the ionizing radiation is inserted into the apparatus. Figure 6 shows the ion distribution after the time of about one second.

Both Figures influence the effect of an external electric field produced by the capacitors in order to separate the ions according to the red curves. As long as the irradiation is present, a stationary state between new production of ions and transport of them to the capacitor plates will be established. A principal difference between the two Figures is an accumulation effect, i.e., the travelling ion concentrations are increased due to the comparably slow diffusion velocity. This property changes the relative amplitude.

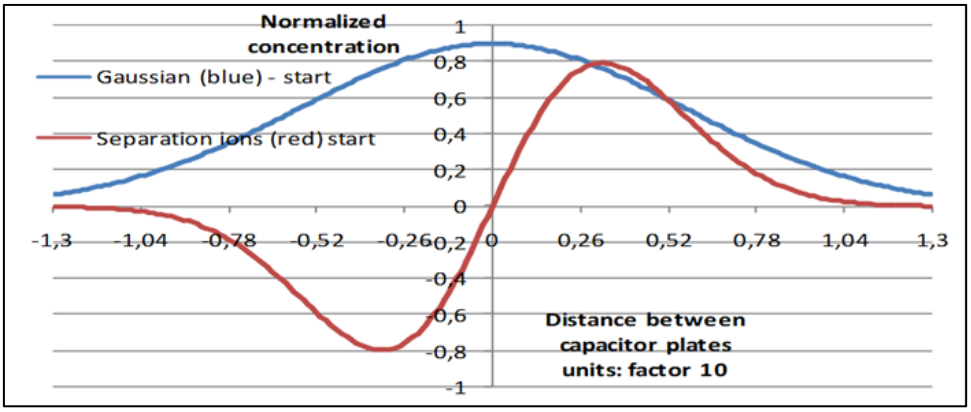

Figure-5. At t = 0 the Gaussian can rather describe the ion distribution (blue), curve red shows the polarization at t = 0

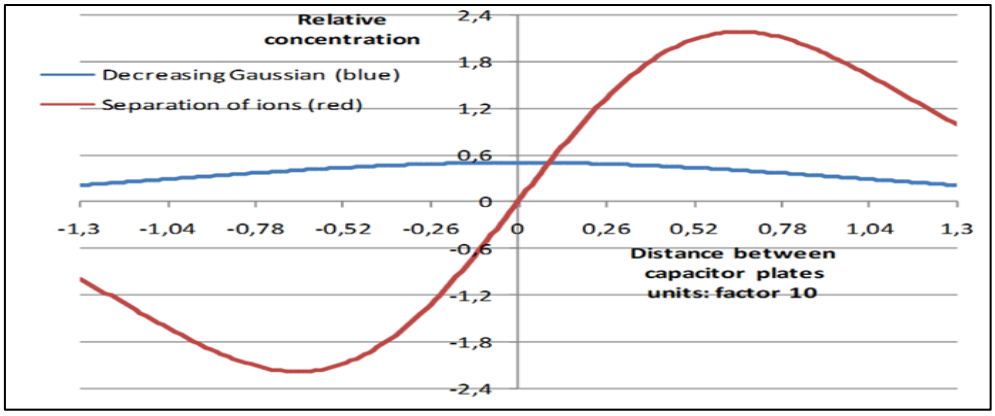

Figure-6. The original Gaussian distribution has nearly been vanished, and the positive ions (positive part of the amplitude) travel in direction to the cathode, whereas the negative ions (negative part of the amplitude) travel in direction to the anode

2.5. Measurement Results

The measurements have been performed with/without irradiation of the phantom, since a comparison of the two the modalities is inevitable.

2.5.1. Description of the Measurement Conditions without Radiation

The described water box contained 2,5 L two-fold distillated water and 50 g NaOH as electrolyte. The outer walls were allocated with 4 solenoid-like electrodes of high-grad steel. The material of the capacitors on both opposite sites were high-grad steel with 1 mm thickness and area of 15 x 10 cm^2. Both, capacitor and solenoids, were supplied with two independent voltage suppliers. It could be verified that a mutual influence existed, i.e., current and voltage could not be controlled of one system without changing the parameters of the other one.

2.5.2 Measurements with Capacitor and Electrodes and Results

The abbreviations in Table 1, Table 2, and succeeding information are: Configuration: Conf.,

E: Electrodes; C: Capacitor; S: Either only capacitor or electrodes are solely involved at measurement process; B: Both capacitor and electrodes are involved, Dose in Gray (Gy), MU: Monitor units per minute.

The results are summarized in Figures 7.1 and 7.2. Figure 7.3 represents a multi regression analysis of the measured data, which incorporate the basis for the Monte-Carlo calculations.

Table-1. Results of the first series without radiation

Voltage/V	Current/A	Conf.	Exposure time H_2O/mL	Deplacement H_2O/mL
3,7	0,79	E	B	B
3,8	1,48	C	8 min	205
3,5	0,34	E	B	B
5,0	2,79	C	5 Min	210
5,9	1,28	E	B	B
8,1	5,16	C	3 Min	210
4,3	0,33	E	B	B
7,4	5,16	C	3 Min 30 sec	200
3,2	0,82	E (S)	8 Min	85
3,4	1,34	C (S)	9 Min	90
7,5	5,16	C (S)	2 Min	200

The measurements with radiation carried out at the Linac have been performed with the following conditions:

Identical experimental conditions for electric supply, concentration of NaOH and two-fold distillated water. Radiation conditions at the Linac: SSD = 90 cm; field size at the isocenter: 10 x 10 cm^2, 6 MV. Dose at entrance: 1,28 Gy and at the end of the water box: 0,7 Gy. The irradiation was performed with three different intensities: 1 Gy (100 monitor units: MU) in one minute, 200 MU in 30 seconds, 3 MU in 20 seconds. The dose intensity in the production of 'Bremsstrahlung' of a Linac is free to be chosen.

All measurement series refer to a field size of 10 x 10 cm^2 and 6 MV. Further details can be taken from the protocol. There are two particular features: The yield of Hydrogen reached the highest value, when the radiation intensity amounted to only 100 MU/min. The augmentation of the radiation intensity to 200 MU/min or 300 MU/min did not deliver the factor two or three with reference to the yield of Hydrogen. The most outstanding result was obtained by a factor of about 9 – 10, when only 100 MU/min two minutes have been exposed, and the identical voltage and current have been used for comparison with absence of radiation (this is the so-called zero experiment).

What can we conclude from these findings? An increase of the radiation intensity requires an increase of the voltage of the power supply in order to attract the ions to the cathode/anode. The four electrodes did only show to

have a local influence, since the results at the case with radiation were nearly identical, when only the capacitor plates were connected to the power supply.

Table-2. Results of the series with radiation

Voltage/V	Current/A	Conf.	Exposure time and MUs/Min	Deplacement H_2O/mL
8,2	5,17	E	1 Min 10 s	B
8,2	6,18	C	100 MUs	260
7,4	5,16	E	1 Min 15 s	B
8,2	5,16	C	100 MUs	245
7,4	6,80	C	1 Min 30 s	B
8,0	5,16	E	100 MUs	330
7,4	6,76	E	90 s	B
8,2	5,16	c	100 MUs, Dose: 300 G/Min	290
7,4	6,73	E	100 MUs Dose: 3 Gy/Min	B
8,2	5,16	C	1 Min 28 s	362
8,2	5,16	C (S)	100 MUs Dose: 1 Gy/Min	310
8,2		C(S)	3 Gy/Min	
8,0	5,16	C(S) 1 Min	100 MUs Dose: 1 Gy/Min	120
3,8	1,28	E (S)	100 MUs 2 Min 10 s	20/25
4,1	1.31	K (S)	100 MUs 2 Min 12 s	195

Conf.	Voltage/V	Current/A	MU per 1 Minute	Total dose in Gy	Displacement per minute: mL / D_L
C	4.02	1.295	100	2	97 (S)
E	4.02	1.295	100	2	11 (S)
C	4.02	1.295	0	0	10 (B)
E	4.02	1.295	0	0	10 (B)
C	8.02	6.82	100	1	445 (B)
E	7.41	5.19	100	1	445(B)
C	8.02	6.82	0	0	66 (B)
E	7.41	5,19	0	0	66 (B)
C	7.42	2.96	0	0	55(B)
E	7.42	2.96	0	0	55(B)
C	7.42	2.96	100	1	336 (B)
E	7.42	2.96	100	1	336 (B)
C	7.42	2.96	0	0	55(B)
E	7.42	2.96	0	0	55(B)
C	7.42	2.96	100	2	320 (B)
E	7.42	2.96	100	2	332 (B)
C	7.42	2.96	0	0	55(B)
E	7.42	2.96	0	0	55(B)

Table-3. Some examples of measurement conditions

Conf.	Voltage/V	Current/A	MU/Min	Dose/Gy	Deplacement mL	Time
C	4,02	1,295	100	2	97	2 Min
E	4,02	1,295	100		11	2 Min
C	8,02	6,82	100	1	445	1 Min
E	7,41	5,19	100	1	445	1 Min
E+C	8,02	6,82	0	0	66	3 Min
E+C	7,41	5,19	0	0	66	3 Min

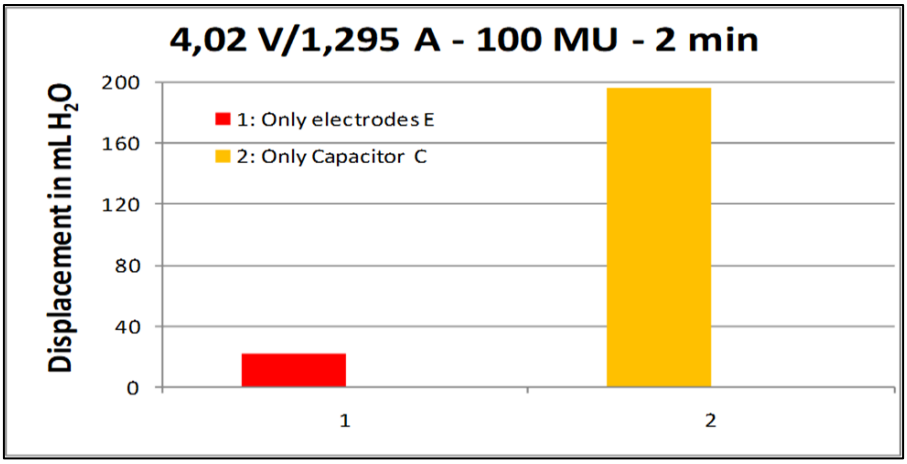

Figure-7.1. Comparison 100 MU: 1 Gy only electrodes (red) and only capacitor (yellow) - this represents the average of one measurement repeated 3 times under the conditions stated in the Figure. The statistical deviations amounted to 1.2 %

2.5.3. Multi Regression Analysis

Dose rate D_R: Number of MUs per minute. The value had to be corrected, because the Linac additionally required always 30 seconds. Gy: The applied dose is always 1 Gy at depth 10 cm (discussed in detail in the description. This statement refers to the delivered total dose! Note: If MU = 0 and dose = 0 then measurement without irradiation

Table-4. Results with irradiation

Conf.	Voltage/V	Current/A	MU per 1 Minute	Total dose in Gy	Displacement per minute: mL / D_L
C	4.02	1.295	100	2	97 (S)
E	4.02	1.295	100	2	11 (S)
C	4.02	1.295	0	0	10 (B)
E	4.02	1.295	0	0	10 (B)
C	8.02	6.82	100	1	445 (B)
E	7.41	5.19	100	1	445(B)
C	8.02	6.82	0	0	66 (B)
E	7.41	5,19	0	0	66 (B)
C	7.42	2.96	0	0	55(B)
E	7.42	2.96	0	0	55(B)
C	7.42	2.96	100	1	336 (B)
E	7.42	2.96	100	1	336 (B)
C	7.42	2.96	0	0	55(B)
E	7.42	2.96	0	0	55(B)
C	7.42	2.96	100	2	320 (B)
E	7.42	2.96	100	2	332 (B)
C	7.42	2.96	0	0	55(B)
E	7.42	2.96	0	0	55(B)
C	742	2.96	100	3	325 (B)
E	7.42	2.96	100	3	325 (B)

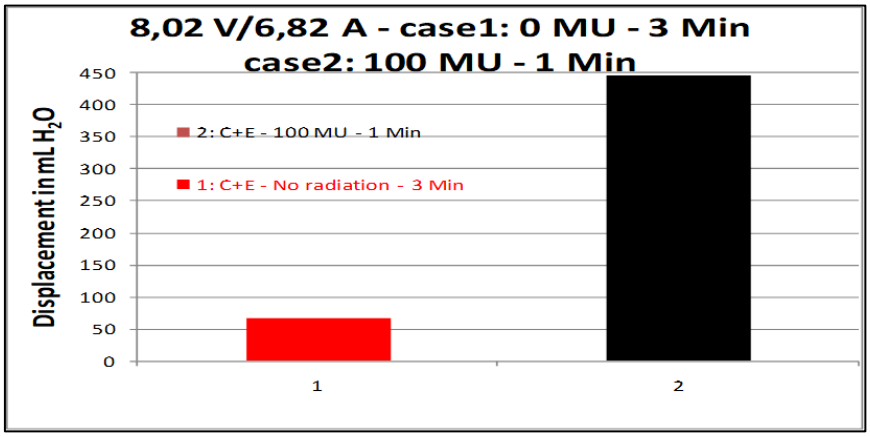

Figure-7.2. Multi-regression analysis - a comparison case 1 (no radiation) and case 2 (radiation)

The multi-regression analysis of the measurement series with and without radiation is present in Figures 7.2 and 7.3.

If the measurement is performed only by one modality of voltage supply (either capacitor or electrodes), then the index S is applied! If the measurement is performed with both modalities, then the index B is used.

All results are uniquely normalized to a one-minute exposure time with and without radiation!

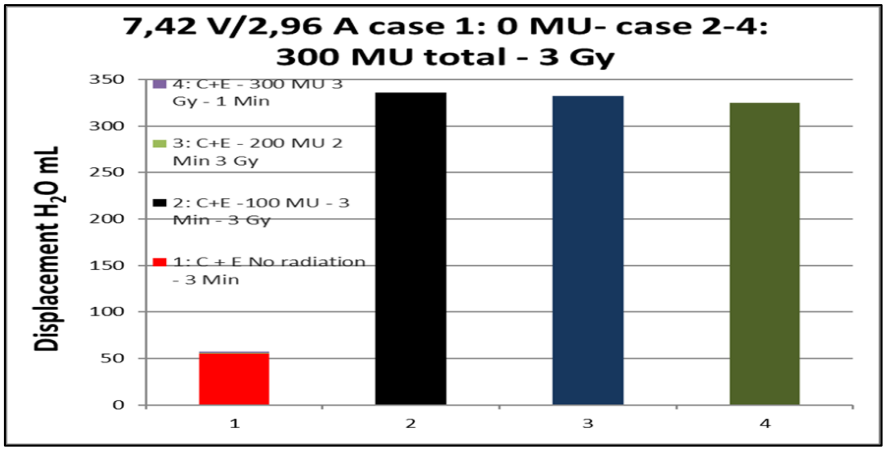

Figure-7.3. Multi-regression analysis: Comparison case 1 no radiation with cases 2 - 4, radiation with different dose rates, total Dose: 3 Gy

2.6. Monte-Carlo Calculation Results with GEANT4

As already pointed, the MC calculations have to account for the geometrical boundaries according to Figure 4 in chapter 2.6, which are given by the propagation of the external radiation in z-direction and the arrangement of the capacitors in perpendicular direction. In order to verify the reliability of the multi-regression analysis, we have used the optimization results according to Figures 7.2. and 7.3. If one regards the depth-dose curve of 6 MV according to Figure 6, one should assume that the output of dose does not have an influence. However, this is not quite correct, since the movability of the ions under an electric field seems to play a certain role, but under the experimental conditions according to the above Figure 7.3 the influence is only of minor importance. Therefore, the MC calculations did not account for this difference. Thus, the deviation in Figures 7.2 amounted to +1.6 % (red case, without irradiation) and +1.9 % (black case, with radiation). In Figure 7.3 we obtained + 1.7 % (red case, without radiation) and + 1.8 % (average of the three cases).

It is noteworthy to mention the modification of the box geometry (material: Lucite instead of aquarium glass) by reduction of the phantom thickness to 5 cm - 6 cm, the capacitor plates are identical and located at the phantom walls, the current and the voltage were reduced to the half compared with the aquarium conditions. By that, the Hydrogen outcome increased by 12 % (red case) and by 13.4 % at the cases with radiation. This difference clearly shows that the mobility of the ions can be exploited in a more suitable way. The commitment of MC calculation appears to represent a useful toolkit in order to reduce experimental trials.

Table-5. Multi regression analysis with and with virtual (MC) radiation, C_MC; Conf.: Configuration

Conf.	Voltage/V	Current/A	MU/related to 1 Minute	Total dose in Gy	Displacement per minute: mL / D_L
C	4.02	1.295	100	2	97
C_MC	4.02	1.295	100	2	95
C	8.02	6.82	100	1	445
C_MC	8.02	6.82	100	1	441
C	7.41	6.82	100	1	370
C_MC	7.41	6.82	100	1	368
C	7.42	2.96	100	2	330
C_MC	7.42	2.96	100	2	328
C	4.42	2.96	100	1	55
C_MC	4.42	2.96	100	1	53
C	7.42	2.96	100	3	325
C_MC	7.42	2.96	100	3	320

Table-6. Multiregression analysis with and with virtual (MC) radiation

Conf.	Voltage/V	Current/A	MU/related to 1 Minute	Total dose in Gy	Displacement per minute: mL / D_L
C	4.02	1.295	100	2	97
C_MC	4.02	1.295	100	2	95
C	8.02	6.82	100	1	445
C_MC	8.02	6.82	100	1	441
C	7.49	6.92	100	1	372
C_MC	7.49	6.92	100	1	370
C	7.42	2.96	100	2	320
C_MC	7.42	2.96	100	2	316
C	4.42	2.96	100	1	55
C_MC	4.42	2.96	100	1	53
C	7.42	2.96	100	3	348
C_MC	7.42	2.96	100	3	346

3. Some Conclusions

A look at Figures 2 and 3 already provides an indication that via reduction of the currents, voltages and the thickness of a phantom this exploitation does not behave in a linear fashion in dependence of the current, voltage and phantom thickness, since all three parameters only show approximately a linear behavior according to the solution function (eq. 15) of the diffusion (eq. 11) extended by an additional electric field. With regard to the use of radioactive waste one has to account for this behavior. The account for the practical feasibility indicates that the phantom thickness only should amount to 5 cm – 6 cm, and the phantom length should be restricted to about 10 cm – 12 cm, if opposite sources consisting mainly of Cs^{137} are taken into consideration. This conclusion is supported by the MC calculations, and this aspect is also considered in the succeeding sections. A significant number of potential improvements and modifications of the present apparatus used in experiments with a Linac are possible. These improvements are sketched in the section 5 (outlook).

4. Outlook

This chapter comprises as a resume the insights received by the measurement conditions and Monte-Carlo calculations. By that, some significant improvements in possible future realizations can be made feasible. Thus, we think about the phantom material and the distance between the capacitor plates.

4.1. Some Feasible Extensions for Technical Applications

4.1.1. Diaphragm

The diaphragm, which separates the anode from the cathode compartments, is necessary in order to separate H_2 from O_2. However, the solution used in these experiments can significantly be improved by semi-permeable walls or layers. Another possibility to reach this separation can be specific layers at the non-return valves.

4.1.2. Electrolytes (Possibly Irrelevant in the Presence of Radiation)

The reported electrolyte for the test measurement was NaOH. In general, bases and H_2SO_4 may be candidates as electrolytes. If H_2SO_4 is considered, then it is necessary that the inner part of the box is equipped with a thin noble metal plate, which is resistant against this acid. HCl must be excluded, because the production of Cl_2 is not desired, and HNO_3 would, besides H_2, also release NH_3. The bases NaOH, KOH, $Mg(OH)_2$, and some other bases in weak or medium concentration are suitable candidates. The effect of these electrolytes on the performance of the cells must be evaluated in the future.

4.1.3. Capacitor Plates

Present experiments have been performed using high-grade steel alloys. The use of copper for long-run applications may be possible, if the electrolytes cannot undergo reactions under radiation conditions. Due to the release of ions in water by radiation exposure, it is possible to avoid electrolytes at all, this property would treat the material with more care. The use of noble metals as capacitor plates is possible, but only a question of costs. Very interesting capacitor plates positioned at the walls are of tungsten or tantalum, but the plates must be isolated from the walls, if the wall material is chosen to be not an insulator. It may be beneficial to use structured plates to increase the active surface area, or deposit co-catalysts on the plates.

4.1.4. Walls of the Aquarium Boxes: Replacement by Lucite

From radiotherapy with protons/photons is known that Lucite is also a very resistant material against ionizing radiation; it is much easier to manipulate mechanically than the Laboratory glass of the used test phantom. The aquarium glass used for phantoms of the tests was easy to purchase, but for technical applications it is not suitable.

4.1.5. Effect of an Inhomogeneous Magnetic (Static) Field

It is well-known that inhomogeneous magnetic fields direct charged particles either to positive or negative directions of their motion. Thus, the poles have to be chosen in a proper way to enhance the transport of H^+ ions to cathode and OH^- ions to anode. An additional influence results from the magnetic interaction with the spin of the particles, and, above all, O_2 is affected by such a field due to its triplet state. This is, however, a second order effect.

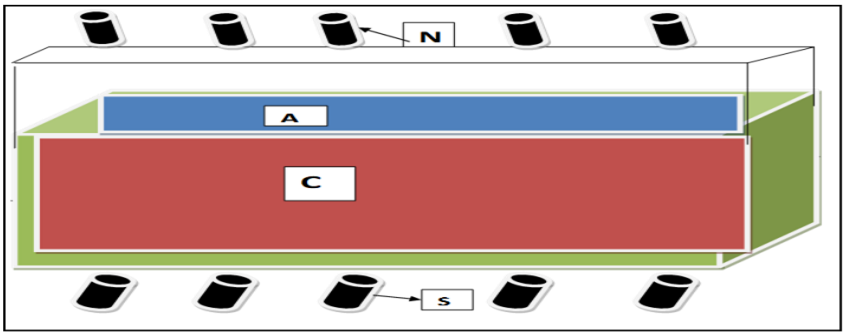

Figure-8. An inhomogeneous magnetic field can enhance the yield of H_2. The magnets with north poles **N** and south poles **S** must possess a bigger extension as show in the above Figure. All magnets are permanent magnets (ferro-magnets) and kept constant by a solenoid. The radiation beam passes between these plates

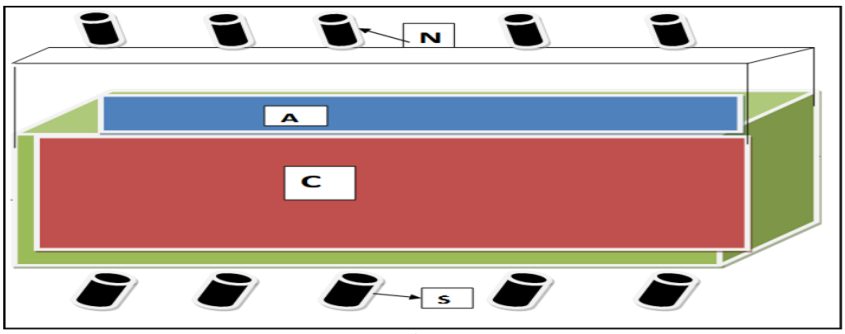

Figure-8a. Instead of the magnet constellation in Figure 8 consisting of single magnets in oblique arrangement it is also possible to apply a long magnet in skew order. The magnet is a permanent magnet (ferro-magnet) and is kept constant by a solenoid. The radiation beam passes between these plates. This is identical with Figure 8

Several boxes consisting of Lucite would be placed in series. They could be separated. As pointed out, the γ-energy of Cs^{137} amounts to 0.7 MeV. This fact implies that a single water box with the length 18 cm is irradiated with a nearly homogeneous dose distribution, if the box is irradiation by an opposite field (one slice of Cs^{137} on each end of the aquarium box). The appropriate voltage depends on the activity and can be reduced in due course. By a measurement and comparison with the Linac results one is able to find the optimum of the voltage. The thickness of the Cs^{137} slices may be of the order of 1 mm -2 mm, placed between the aquarium boxes. The complete arrangement is shown in Figure 8, but the number of aquarium boxes is not restricted by the drawing and may enormously be stretched. Thus about 100 cells in one sequence require a length of ca. 18 m – 19 m. It is also obvious that such an arrangement of 'cells' for the gas production requires remote and control implementations in order to survey all functions and to satisfy the radiation protection.

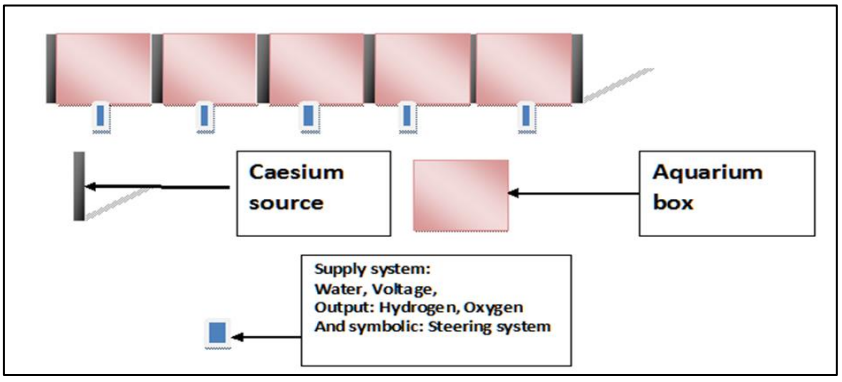

Figure-9. Model of a sequence of phantom cells for the production of H_2 and O_2

5. Monte Carlo Calculations of a Phantom with Reduced Thickness Diameter

We have already pointed out in previous sections that with regard to have an available phantom for some experimental tests a phantom consisting of laboratory glass and fixed phantom extensions. The most important feature is the increase of the electric field strength E = U/d by reduction of the phantom breath. In order to receive the identical output, the corresponding parameters of the voltage and current can be significantly reduced according

to Table 7. Abbreviation: ***dm*** is the diameter of the phantom breadth. The sequence of parameters agrees with those in Tables 5 and 6.

Table-7. Multi regression analysis with virtual (MC) radiation with phantom diameters dm = 13 cm referred to as **C_MCp** with dm = 13 cm and to as **C_MC**_ with dm = 5 cm.

Monte-Carlo Conf.	Voltage/V	Current/A	MU in 1 Minute	Dose in Gy	Displacement per minute: mL / D_L	Phantom diameter
C_MCp	5.02	1.295	100	2	125	dm: 13 cm
C_MC	1.79	1.295	100	2	125	dm: 5 cm
C_MCp	8.02	6.82	100	1	441	dm: 13 cm
C_MC	3.13	2.44	100	1	441	dm: 5 cm
C_MCp	7.41	6.82	100	1	320	dm: 13 cm
C_MC	2,90	2,32	100	1	312	dm: 5 cm
C_MCp	7.42	2.96	100	2	320	dm: 13 cm
C_MC	2,93	1,09	100	2	312	dm: 5 cm
C_MCp	4.42	2.96	100	1	53	dm: 13 cm
C_MC	1,73	1,12	100	1	53	dm: 5 cm
C_MCp	7.42	2.96	100	3	346	dm: 13 cm
C_MC	1,75	1,16	100	3	346	dm: 5 cm

The Monte-Carlo calculations provide a clear insight that a measurement configuration with dm = 5 cm (y-axis) imply a significant improvement by this reduction of the phantom thickness. This knowledge confirms the conjecture that this improvement results from the consequence of the electric field strength **E**, which is increased by a diminution of the distance dm between the capacitors according to the relation $\mathbf{E_y = U/dm}$.

5.1. Use of Radioactive Decay Products of Nuclear Reactors

The half-time of Cs^{137} amounts to about 30 years. Therefore, there are attempts that it can be handled by usual technical methods. In order to avoid this long-time and unpredictable storage, there have been elaborated some concepts, which all can be referred to as ***'transmutations'***. These concepts mainly deal with further irradiation of the decay products such as Cs^{137} via fast neutrons in similar way as the nuclear reactors work with U^{235} or similar appropriate nuclei. However, it is not clear how to apply the released energy and what is the amount of the energy to make the transmutations realistic [7 - 9]. Besides the neutron path we may also think of irradiation with protons, since such installations are becoming rather wide-spread due to improvements in radiotherapy with protons. Two typical reactions of protons with Cs^{137} are stated by eq. (2) and eq. (3):

$$p + Cs_{55}^{137} \rightarrow p + n + Cs_{55}^{136} + \gamma \quad (17)$$

$$p + Cs_{55}^{137} \rightarrow n + Ba_{56}^{137} \quad + \gamma \quad (18)$$

The two reactions with protons deserve particular interest, because according to eq. (2) another Cs-isotope is produced with a half-time of about 22 days in contrast to the 30 years of Cs^{137} . The keywords '***Radioactive waste – new exploitation technologies'*** provide various references in the internet, a listing of them seems not to be necessary.

We have to point out that the goal of this study is the enormous source of radiation energy resulting as decay products (radioactive waste) of nuclear reactors after separation of U_{235} and Plutonium, which both are made again applicable for new fission processes (this procedure is performed in a so-called reprocessing plant). Relations (9, and 10) show possible nuclear reactions of Cs^{137} irradiated with protons. Thus eq. (9) would provide a rather nice reaction product, namely Cs^{136} with a half-time of about 22 days [7-9]. The second possible reaction referred to as equation (10) with protons delivers the element Barium, which is a stable metal. Thus, the energy of the proton must not exceed 70 MeV in order to enable the above nuclear reactions and to prevent other undesired nuclear processes. The relationship between the required proton energy and the released γ-quanta is also an open question, because the principal way how to exploit the γ-energy according to the above equations 9 and 10 is also not yet elaborated. Nevertheless, it may be possible and useful to combine a transmutation technology with the method of enhanced Hydrogen production by exploiting the γ-radiation of radioactive decay products of nuclear reactors.

With regard to nuclear reactions occurring in reactors it should be recalled that a nuclear fission induced by a neutron collision with U^{235} (or a similar nucleus such as Plutonium) usually produces two fission nuclei with about the half mass of the origin nucleus. Therefore, the most important fission products are the isotopes: Cesium, Barium, Strontium, but also Co^{60} and Iodine. Thus, only Iodine isotopes exhibit a rather short half-time, and, by that, they are not a problem with regard to radioactive waste. As already pointed out, Cs^{137} represents the most outstanding fission product.

As pointed out, the γ-energy of Cs^{137} amounts to 0.7 MeV. This fact includes, that a water box with the length 18 cm is irradiated with a nearly homogeneous dose distribution, if the box is irradiation by an opposite field (one slice of Cs^{137} on each end of the aquarium box). The appropriate voltage depends on the activity and can be reduced in due course. By a measurement and comparison with the Linac results one is able to find the optimum of the voltage. The thickness of the Cs^{137} slices may be of the order of 1 mm, placed at the walls between the aquarium boxes. The complete arrangement is shown in Figure 9, but the number of aquarium boxes is not restricted by the drawing and may enormously be stretched. Thus about 100 cells in one sequence require a length of ca. 18 m – 19 m. It is also obvious that such an arrangement of 'cells' for the gas production requires remote, and control

implementations in order to survey all functions and to satisfy the radiation protection. It is also a result of the Monte-Carlo studies, that a reduction of the phantom thickness increases the electric field strength between the capacitors and the yield of H_2 can significantly be improved. The present study provides a clear indication that the storage of radioactive waste in bunkers without exploiting the radiation energy incorporates wastages of natural resources in view of the actual necessity of receiving new energy sources.

Acknowledgement

The authors thank Dipl.-Ing Uwe Wild for making experimental tests of the theoretical results at the Radio-Oncology Center, Maximilienplatz, Munich possible.

References

[1] Ulmer, W., Pyyry, J., and Kaissl, A. W., 2005. "3D photon superposition/convolution algorithm and its foundation on results of Monte Carlo calculations." *Physics in Medicine and Biology*, vol. 50, pp. 1767-1790.

[2] "Collection of projects in US of Hydrogen-production-electrolysis." Available: https://www.energy.gov/eere/fuelcells/Hydrogen-production-electrolysis

[3] Walter, M. G., Warren, E. L., McKone, J. R., Boettcher, S. W., Mi, Q., Santori, E. A., and Lewis, N. S., 2010. "Solar water splitting cells." *Chem. Rev.*, vol. 110, pp. 6446-6473.

[4] Kato, H., Asakura, K., and Kudo, A., 2003. "Highly efficient water splitting into h-2 and o-2 over lanthanum-doped natao3 photocatalysts with high crystallinity and surface nanostructure." *J. Am. Chem. Soc.*, vol. 125, pp. 3082-3089.

[5] GEANT4-Documents, 2005. Available: http://geant4.web.cern/geant4/G4UsersDocuments/Overview/html/S

[6] Ulmer, W., 1985. "On a unified treatment of kinetics and diffusion, and a connection to a nonlocal Boltzmann equation." *Int. Journal of Quantum Chemistry*, Available: https://doi.org/10.1002/qua.560270211

[7] Kulke, U., 2010. "Atommüll wird in 20 Jahren nicht mehr sein, Tageszeitung." *Die Welt*, p. 9.

[8] Etspüler, M., 2012. *Die entschärfung des atommülls* vol. 25. Wissen and Umwelt, DW, p. 4.

[9] Ulmer, W., 2016. "Characterization of specific nuclear reaction channels by deconvolution in the energy space of the total nuclear cross-section of protons-applications to proton therapy and technical problems (transmutations)." *Journal of Proton Therapy*, vol. 2, p. 212.